Published in final edited form as:
Neuron. 2013 September 4; 79(5): 887–902. doi:10.1016/j.neuron.2013.06.036.

Metabotropic Glutamate Receptor 5 is a Co-Receptor for Alzheimer Aβ Oligomer Bound to Cellular Prion Protein

Ji Won Um[1], **Adam C. Kaufman**[1], **Mikhail Kostylev**[1], **Jacqueline K. Heiss**[1], **Massimiliano Stagi**[1], **Hideyuki Takahashi**[1], **Meghan E. Kerrisk**[2], **Alexander Vortmeyer**[3], **Thomas Wisniewski**[4], **Anthony J. Koleske**[2], **Erik C. Gunther**[1], **Haakon B. Nygaard**[1], and **Stephen M. Strittmatter**[1]

[1]Cellular Neuroscience, Neurodegeneration and Repair Program, Departments of Neurology and Neurobiology, Yale University School of Medicine, New Haven, CT 06536 USA

[2]Department of Molecular Biophysics and Biochemistry, Yale University School of Medicine, New Haven, CT 06536 USA

[3]Department of Pathology, Yale University School of Medicine, New Haven, CT 06536 USA

[4]Department of Neurology, New York University School of Medicine, 550 First Avenue, New York, NY 10016, USA

SUMMARY

Soluble Amyloid-β oligomers (Aβo) trigger Alzheimer's disease (AD) pathophysiology and bind with high affinity to Cellular Prion Protein (PrP^C). At the post-synaptic density (PSD), extracellular Aβo bound to lipid-anchored PrP^C activates intracellular Fyn kinase to disrupt synapses. Here, we screened transmembrane PSD proteins heterologously for the ability to couple Aβo–PrP^C with Fyn. Only co-expression of the metabotropic glutamate receptor, mGluR5, allowed PrP^C-bound Aβo to activate Fyn. PrP^C and mGluR5 interact physically, and cytoplasmic Fyn forms a complex with mGluR5. Aβo–PrP^C generates mGluR5-mediated increases of intracellular calcium in *Xenopus* oocytes and in neurons, and the later is also driven by human AD brain extracts. In addition, signaling by Aβo–PrP^C–mGluR5 complexes mediates eEF2 phosphorylation and dendritic spine loss. For mice expressing familial AD transgenes, mGluR5 antagonism reverses deficits in learning, memory and synapse density. Thus, Aβo–PrP^C complexes at the neuronal surface activate mGluR5 to disrupt neuronal function.

INTRODUCTION

Alzheimer's disease (AD) has a distinct pathology with plaques of amyloid-β (Aβ) and tangles of hyperphosphorylated tau. Rare autosomal dominant AD cases with mutations of Amyloid-β Precursor Protein (APP) or Presenilin (PS1 or PS2) provide proof that Aβ pathways can trigger AD (reviewed in (Holtzman et al., 2011)). Other APP mutations reduce AD risk (Jonsson et al., 2012). Biomarker studies of late onset AD have shown that Aβ dysregulation, detected by CSF levels or by PET, is the earliest detectable change, consistent with Aβ as a trigger (Holtzman et al., 2011).

Correspondence and requests for materials should be addressed to S.M.S. (stephen.strittmatter@yale.edu).

The mechanism whereby Aβ leads to AD is less clear. Attention has focused on soluble oligomers of Aβ (Aβo) as causing synaptic malfunction and loss of dendritic spines (Shankar et al., 2008). In the only reported genome-wide unbiased screen for Aβo binding sites, we identified PrP^C (Lauren et al., 2009). Aβ binding to PrP^C is high affinity and oligomer specific (Chen et al., 2010; Lauren et al., 2009). *In vivo*, PrP^C is not essential for certain Aβ-related phenotypes, but is required for cell death *in vitro*, for reduced survival of APP/PS1 transgenic lines, for epileptiform discharges, for synapse loss, for serotonin axon degeneration and for spatial learning and memory deficits (reviewed in (Um and Strittmatter, 2013)). Critically, the ability of human AD brain-derived Aβ species to suppress synaptic plasticity requires PrP^C, and human AD brain contains PrP^C-interacting Aβo and Aβ–PrP^C complexes (Barry et al., 2011; Freir et al., 2011; Um et al., 2012; Zou et al., 2011).

Aβo–PrP^C complexes signal to intracellular Fyn kinase (Larson et al., 2012; Um et al., 2012). PrP^C phenotypes in fish and worm require Fyn (Bizat et al., 2010; Malaga-Trillo et al., 2009), Fyn regulates Glu receptor traffic and plasticity (Grant et al., 1992; Prybylowski et al., 2005), and Fyn interacts with tau (Ittner et al., 2010; Roberson et al., 2011). Both PrP^C and Fyn are enriched in the Post-Synaptic Density (PSD), and Aβo engagement of PrP^C activates Fyn to phosphorylate NMDA receptors (Larson et al., 2012; Um et al., 2012).

The connection from Aβo–PrP^C complexes to Fyn cannot be direct, because PrP^C is anchored via glycolipid to the plasma membrane while Fyn is cytoplasmic. Since both are enriched in PSDs (Collins et al., 2006; Um et al., 2012), we hypothesized that a transmembrane PSD protein might couple PrP^C with Fyn. The PSD proteome includes 81 transmembrane proteins (Collins et al., 2006; Emes et al., 2008). Here, we screened PSD transmembrane proteins for their ability to couple Aβo–PrP^C with Fyn. We identified mGluR5 as linking PrP^C to Fyn. Activation of neuronal Fyn requires both mGluR5 and PrP^C. Aβo–PrP^C can drive mGluR5-dependent calcium mobilization and eEF2 phosphorylation. Antagonists of mGluR5 prevent Aβo-induced dendritic spine loss and AD transgene learning and memory deficits. These studies define an Aβo–PrP^C–mGluR5 complex that leads to impaired neuronal function.

RESULTS

Screen for PSD Proteins Mediating Aβo/PrP^C Signaling Identifies mGluR5

We considered the 81 known transmembrane PSD proteins as potential mediators (Fig. 1A, B). We utilized a cell type in which PrP^C and Fyn fail to couple. When PrP^C and Fyn are overexpressed in HEK293T cells, Aβo does not activate Fyn, as in neurons (Um et al., 2012). We co-expressed PSD proteins together with PrP^C and exposed the HEK cells to Aβo prior to assessing Fyn activation by anti-phospho-SFK (Src Family Kinase) immunoblot (Fig. 1B–D). In addition to 56 documented PSD proteins, we included APLP1 and APLP2, due similarity with the PSD protein, APP, and known interaction with PrP^C or Aβo (Bai et al., 2008; Lauren et al., 2009; Schmitt-Ulms et al., 2004). We included the LRRTM family because they organize synapses and modify Aβ levels (Linhoff et al., 2009; Majercak et al., 2006). Of 61 proteins screened, only mGluR1 and mGluR5 increased Fyn activation by more than two standard deviations (Fig. 1C, D). mGluR5 is reported to co-immunoprecipitate and activate Fyn (Heidinger et al., 2002), to redistribute after Aβo (Renner et al., 2010), to co-localize with Aβo (Renner et al., 2010), and to be required for Aβo suppression of LTP (Rammes et al., 2011; Shankar et al., 2008; Wang et al., 2004).

In the initial screen with Aβo, mGluR1 or mGluR5 activity might have been ligand-dependent or independent. While co-expression of either receptor results in baseline activation of Fyn, only mGluR5 mediates Aβo activation (Fig. 1E–G). Neuronal Aβo-

induced Fyn activation is PrP^C–dependent, as for neurons (Um et al., 2012), because when mGluR5 is expressed without PrP^C, no Aβo regulation of Fyn occurs. In contrast, basal Fyn activity (without Aβo) is independent of PrP^C and equal for mGluR1 and mGluR5. Thus, mGluR5 alone has the property of mediating Aβo–PrP^C activation of Fyn in HEK cells.

Although EphB2 is not a PSD consensus member, we considered EphB2 as a link between Aβo and Fyn because it couples with Fyn during development, and because Aβ alters EphB2 level (Cisse et al., 2011; Takasu et al., 2002). In HEK, co-expression of EphB2 and Fyn yields kinase activation (Takasu et al., 2002), but EphB2 does not mediate Aβo signaling (Suppl. Fig. S1).

We sought to determine if neuronal mGluR5 is required for Aβo-induced Fyn activation. The mGluR5 negative allosteric modulator, MPEP, blocks Aβo-induced Fyn activation in HEK cells (Fig. 1E) so we preincubated cortical neurons with MPEP, or the related MTEP, prior to Aβo (Fig. 1H, J). Neither MTEP nor MPEP alters baseline Fyn activity, but both eliminate Aβo-induced activation. The mGluR1 antagonist, MPMQ, does not prevent Aβo-induced Fyn activation (Fig. 1H, J). We also cultured *Grm5*−/− cortical neurons and exposed them to Aβo at 21DIV (Fig. 1I, J). Under basal conditions, phospho-Fyn levels were similar to WT, but the increase by Aβo was eliminated. Thus, mGluR5, as well as PrP^C, is required for this Aβo signal transduction.

mGluR5 does not bind Aβo, but Physically Associates with PrP^C and Fyn

With evidence that PrP^C, mGluR5 and Fyn participate in Aβo signaling, we assessed physical interaction amongst them. We visualized Aβo binding to COS-7 cells expressing mGluR5, PrP^C, both or neither (Fig. 2A, B). Aβo binding to PrP^C-expressing cells is not altered by mGluR5, and there is no detectable binding of Aβo to mGluR5 without PrP^C. PrP^C alone accounts for Aβo surface binding.

If mGluR5 serves as a bridge between PrP^C and Fyn, then it is predicted to interact physically with both. We confirmed an association of mGluR5 with Fyn (Heidinger et al., 2002), and observed no alteration by PrP^C or Aβo (Suppl. Fig. 2A). Both mGluR1 and mGluR5 associate with Fyn, but mGluR8 does not (Suppl. Fig. 2B). In HEK293T cells, PrP^C immunoprecipitates contain mGluR5, regardless of Aβo (Fig. 2C). Both mGluR1 and mGluR5, but not mGluR8, co-immunoprecipitate with PrP^C (Fig. 2D). We utilized this specificity to examine whether discrete mGluR5 domains are responsible for PrP^C interaction (Suppl. Fig. 2C). Chimeric proteins containing the N-terminal globular domain from one mGluR fused to the transmembrane domains from another mGluR were co-expressed with PrP^C. Each chimera co-immunoprecipitates PrP^C less effectively than mGluR5 (Suppl. Fig. 2D), suggesting that the PrP^C–interacting regions are distributed in the protein.

In brain, mGluR5 and PrP^C are co-enriched in detergent-resistant PSD fractions (Fig. 2E) (Collins et al., 2006; Um et al., 2012). To assess association of endogenous proteins extractable with non-denaturing detergent, we covalently cross-linked proteins and then precipitated PrP^C. The PrP^C immunoprecipitates contain mGluR5, but not mGluR8, NR2B or GluR1 (Fig. 2F). Immunoprecipitates from *Prnp*−/− samples do not exhibit mGluR5. Thus, Aβo–PrP^C, PrP^C–mGluR5, mGluR5–Fyn pairwise physical associations are detectable.

To evaluate PrP^C specificity for mGluR5, we applied soluble PrP^C as a ligand to mGluR5-expressing cells. PrP-His binds more avidly to COS-7 cells expressing mGluR5 than to non-transfected or mGluR1-expressing or mGluR8-expressing cells (Suppl. Fig. S2E, F). Thus, in this more stringent test of protein interaction, mGluR5, but not mGluR1 or mGluR8, has

affinity for PrP^C. We utilized similar conditions to examine soluble PrP^C binding to neurons with a human-specific anti-PrP^C to selectively visualize immunoreactivity of the recombinant ligand (Fig. 2G, H). Punctate binding of soluble PrP^C along dendrites is visible (Fig. 2G). This staining is reduced by 70% in *Grm5*−/− cultures, with the remaining signal similar to the non-specific low-affinity level observed in non-transfected COS-7 cells (Supp. Fig. S2E, F). We conclude that mGluR5 contributes significantly as a PrP^C partner on the neuronal surface.

Expression of PrP^C plus mGluR5 Supports Aβo-Induced Increase of Intracellular Calcium

Activation of Fyn is one consequence of mGluR5 engagement, but activation of the heterotrimeric GTPases, G_q/G_{11}, with subsequent production of inositol (3,4,5) trisphosphate (IP3) and release of intracellular calcium, is the more prominent pathway (Luscher and Huber, 2010). We considered whether Aβo–PrP^C might activate this pathway by injecting RNA for mGluR5 and PrP^C into *X. laevis* oocytes and applying a two-electrode voltage clamp during bath perfusion of Aβo. G protein activation of phospholipase C leads to IP3, calcium release and opening of an easily detected transmembrane chloride channel in oocytes (Saugstad et al., 1996; Strittmatter et al., 1993). Glu-induced responses of 3000 nA peak current at -60 mV are detected in oocytes expressing mGluR1 or mGluR5 (Fig. 3A, B). PrP^C does not alter the Glu responses. Bath application of Aβo had no effect on conductances for uninjected oocytes, or oocytes expressing mGluR5 alone or PrP^C alone (Fig. 3C). However, in the double-expressing mGluR5-PrP^C oocytes, Aβo produced an inward current of 300–450 nA, 10% of the Glu-induced current. We included only mGluR oocyte batches with Glu responses greater than 500 nA. For preparations with less than 500 nA responses to Glu, Aβo responses of 10% Glu magnitude may be present, but are not prominent. The kinetics and reversal potential for the Aβo-induced signal were indistinguishable from that of Glu acting on mGluR5 alone (Fig. 3A and not shown).

The specificity of the Aβo-induced current of PrP^C–mGluR5 oocytes was examined. While mGluR1 expression leads to equally strong Glu-induced current (Fig. 3A, B), there is no detectable Aβo-induced current (Fig. 3A, C). PrP^C lacking the Aβo binding domain, PrPΔ23-111 (Chen et al., 2010; Lauren et al., 2009; Um et al., 2012), fails to support Aβo-induced signaling through mGluR5 (Fig. 3C). The anti-PrP^C antibody, 6D11, binds to residues 95–105 and prevents Aβo interaction (Chung et al., 2010; Lauren et al., 2009; Um et al., 2012). Preincubation with 6D11 blocks Aβo responses, but not Glu responses, in PrP^C-mGluR5 oocytes (Fig. 3B, C). The Aβo–induced response has an EC50 of 1 μM monomer equivalent, an estimated 10 nM oligomer concentration (Fig. 3D). A characteristic of G protein mediated responses in *Xenopus* oocytes is strong desensitization. Maximal Glu stimulation nearly eliminates subsequent responses to Glu for 10–15 min. Consistent with the Aβo–PrP^C–mGluR5 responses sharing this pathway, pretreatment with Glu eliminates the response to subsequent Aβo (Fig. 3E). In addition, pretreatment with cell permeable BAPTA-AM to chelate intracellular calcium abrogated the Aβo-induced signal (Fig. 3E), as for Glu (Saugstad et al., 1996). Thus, Aβo interaction with a PrP^C–mGluR5 complex mobilizes calcium stores. While mGluR5-mediated signaling to Fyn is as robust with Aβo–PrP^C as with Glu, signaling to calcium mobilization is substantially less effective for Aβo–PrP^C than with Glu as the mGluR5 ligand, so Aβo does not mimic Glu precisely.

Acute Aβo-Induced Calcium Signals in Neuronal Culture Require mGluR5 and PrP^C

We considered whether Aβo regulates neuronal calcium signaling through mGluR5 directly and acutely. Chronic Aβo–PrP^C–Fyn signaling can indirectly alter NMDA-R trafficking to modulate NMDA-induced calcium responses (Um et al., 2012). We used a calcium-sensitive fluorescent dye to assess direct immediate response to Aβo in 21DIV cortical cultures. In low-density cultures, there is little direct calcium response to Aβo under the conditions that

modulate NMDA-R responses (not shown and (Um et al., 2012)). With microscopic imaging, Aβo occasionally induces local calcium transients, but there is no generalization and measurement across a microtiter well does not detect a change (not shown). Higher density cultures exhibit spontaneous synchronized calcium increases (Suppl. Fig. S3A) that depend on network connectivity being suppressed by TTX, CNQX, or APV (Suppl. Fig. S3B, C) (Dravid and Murray, 2004). Under these conditions, Aβo induces an increase of intracellular calcium (Fig. 4A). Averaging multiple wells smoothes random spontaneous signals (Suppl. Fig. S3A), and Aβo-induced responses are apparent (Fig. 4A). This response is oligomer specific; no response is detected with monomeric Aβ (Fig. 4C). In either *Grm5*−/− or *Prnp*−/− neurons, the spontaneous synchronized calcium signals are indistinguishable from WT (Suppl. Fig. S3D, E). However, Aβo fails to induce a calcium signal in networks lacking either PrP^C or mGluR5 (Fig. 4B).

To assess whether similar responses occur with human autopsy tissue, we utilized TBS-soluble extracts from human brain, which we have previously characterized for PrP^C–interacting Aβ species and for Fyn activation in mouse cultures (Suppl. Table S1 and (Um et al., 2012)). In high-density cortical cultures, dialyzed TBS-soluble brain extracts from AD cases generate greater calcium mobilization than do Control brain extracts (Fig. 4D, E; $P<0.001$). Moreover, the level of PrP(23-111)-interacting Aβ in human brain samples correlates with the magnitude of the calcium response (Fig. 4F). Pre-absorption with anti-Aβ antibody removes PrP^C-interacting Aβ immunoreactivity (Suppl. Fig. S3H) and reduces the calcium response (Suppl. Fig. S3F, G). Preabsorption with PrP-Fc, but not control Fc resin, removes PrP^C-interacting species and reduces the calcium response (Fig. 4G, Suppl. Fig. S3I). Thus, PrP^C–interacting Aβ species in human AD brain TBS-soluble extracts stimulate calcium signals in high-density neuronal cultures. These responses require network connectivity, and are blocked by TTX, CNQX or APV (Suppl. Fig. S4J). The mGluR5 antagonists, MPEP and MTEP, block the AD brain extract response (Fig. 4I). In contrast, the mGluR1 antagonist MPMQ does not block the AD extract-induced response (Fig. 4I). Furthermore, the ability of human AD brain extract to induce a calcium signal is eliminated in *Grm5*−/− or *Prnp*−/− neurons (Fig. 4H).

We considered the source of calcium for the AD extract-induced signal and its relationship to Fyn. Thapsigargin (TG) pretreatment prevented signaling, consistent with release from endoplasmic reticulum stores (Fig. 4I). In contrast, TG pretreatment did not prevent Fyn activation (Fig. 4J, K) and inhibition of Fyn with saracatinib did not prevent calcium signaling (Fig. 4I). While Fyn and calcium signaling by AD extracts require both PrP^C and mGluR5, the two mediators appear pharmacologically separable.

Chronic Aβo has the potential to desensitize mGluR5 calcium responses. We assessed this in two models: HEK293 cells expressing mGluR5 and PrP^C, and low density cultured neurons. HEK–mGluR5 cells respond to Glu with calcium elevation and there is no effect of Aβo pre-incubation (Supp. Fig. S4A, B, F). For HEK cells stably expressing mGluR5 and PrP^C, baseline Glu responses are similar, but Aβo preincubation suppresses Glu responses by 50% in independent clones (Suppl. Fig. S4A, C, D, F). This effect requires the Aβo-binding PrP(23-111) domain because clones expressing a truncation mutant fail to bind Aβo (Suppl. Fig. S5A), and show no Aβo suppression of Glu-induced calcium (Suppl. Fig. S4E, F). Aβo-induced suppression of mGluR5 responses is also observed in neurons. In low density cultures, there are no spontaneous synchronized calcium oscillations, but the mGluR5 agonist, DHPG, results in synchronized oscillations (Suppl. Fig. S4G). Pretreatment with Aβo nearly eliminates DHPG-induced oscillations in WT neurons (90% inhibition, Suppl. Fig. S4H, I). The Aβo suppression of DHPG-induced oscillations is limited to 40% in *Prnp*−/− cultures (Suppl. Fig. S4I).

Multiple mechanisms contribute to mGluR5 desensitization, including protein kinase C, calcium/calmodulin binding and receptor internalization. We assessed the effect of Aβo and the group I mGlu receptor agonist, DHPG, on cell surface mGluR5 levels using biotinylation of live neurons with a cell impermeable reagent (Suppl. Fig. S4J–L). At 1 hour, DHPG reduces surface mGluR5 by 20%, as described (Choi et al., 2011). In contrast, Aβo treatment generates a PrP^C-dependent 25% *increase* in surface/total mGluR5 ratios (Suppl. Fig. S4J–L). The increase after Aβo addition may reflect "trapping" of mGluR5 in relatively immobile complexes (Renner et al., 2010). Despite this difference between Aβo and DHPG in mGluR5 trafficking, Aβo treatment suppresses mGluR5 signaling (Suppl. Fig. S4H, I).

Aβo Signals through PrP^C and mGluR5 to Protein Translation Machinery

Metabotropic GluRs have effects on protein translation (Luscher and Huber, 2010), as well as calcium release and Fyn. We examined whether Aβo–PrP^C–mGluR5 coupling might alter phosphorylation of eukaryotic elongation factor 2 (eEF2). The mGluR5 agonist, DHPG, drives eEF2-56T phosphorylation (Suppl. Fig. S5A). Aβo treatment has a similar effect on eEF2 phosphorylation (Fig. 5A, B, Suppl. Fig. S5A–C). Mediation of the Aβo effect by mGluR5 is demonstrated by inhibition with MTEP (Suppl. Fig. S5B, C). In contrast, the mGluR1 antagonist, MPMQ, does not prevent Aβo-induced eEF2 phosphorylation (Suppl. Fig. S5D, E). Genetic analysis with *Prnp*−/− and *Grm5*−/− neurons confirms that the Aβo effect on eEF2 phosphorylation depends on these proteins (Fig. 5A, B). Aβo-induced eEF2 phosphorylation is detected in dendrites, and is absent in *Prnp* −/− and *Grm5* −/− neurons (Fig. 5C, D). The addition of both Aβo and DHPG produced no greater eEF2 phosphorylation than either ligand alone, consistent with occlusive action (Suppl. Fig. S5F, G).

Dendritic translation of Arc is under mGluR5 control, via an eEF2-dependent mechanism (Park et al., 2008). As predicted from the mGluR5-mediated action of Aβo on p-eEF2, dendritic Arc immunoreactivity is elevated after 5 min Aβo exposure (Fig. 5E, F) and Arc immunoblot signal increases in brain slices (Suppl. Fig. S5H, I).

To extend the AD relevance of these observations, we tested whether human AD extracts generated a similar pattern. Pooled TBS-soluble extracts from AD brain, but not Control brain, elevated eEF2 phosphorylation in WT mouse 21DIV neurons (Fig. 5G, H). This signaling is not observed in *Grm5*−/− and *Prnp*−/− cultures. Thus, Aβo–PrP^C complexes signal through mGluR5 to modify Fyn activation, calcium levels and eEF2 phosphorylation.

We considered how Aβo-induced eEF2 phosphorylation relates to Fyn activation and calcium signaling. Saracatinib suppresses basal p-SFK levels and prevents Aβo stimulation of Fyn (Fig. 5I), and also prevents Aβo-induced eEF2 phosphorylation (Fig. 5I, K). Thapsigargin pretreatment prevents AD extract-induced calcium signaling (Fig. 4H), and also prevents eEF2 phosphorylation (Fig. 5J, K). Thus, eEF2 regulation by Aβo requires both Fyn and calcium signaling.

Cellular Effects of Aβo Require mGluR5

Time-lapse imaging of myristoyl-GFP expressing neurons (Fig. 6A) has shown that Aβo leads to a loss of 10% of dendritic spines over 5 hours by a *Prnp*– and *Fyn*–dependent mechanism (Um et al., 2012). Acute DHPG treatment leads to immature spines, reduced spine volume and fewer surface AMPA receptors during chemical LTD (Abu-Elneel et al., 2008; Moult et al., 2006; Vanderklish and Edelman, 2002), while chronic DHPG results in decreased spine density (Shinoda et al., 2010). We tested whether mGluR5 blockade prevents Aβo-induced spine loss. MPEP treatment does not alter baseline spine stability over 5 h, but prevents Aβo–induced loss (Fig. 6A, B). Deletion of mGluR5 also prevents Aβo-

induced spine loss (Fig. 6A, C). Thus, mGluR5 participates in morphological effects of Aβo–PrP^C complexes.

The Aβo–PrP^C–Fyn pathway contributes to short-term LDH release from neurons (Um et al., 2012). Either addition of the mGluR5 negative allosteric modulator, MTEP, or deletion of the *Grm5* gene prevents Aβo-induced LDH release (Fig. 6D, E).

mGluR5 Antagonist Reverses Behavioral Deficits in FAD Transgenic Mice

The double transgenic APPswe/PS1ΔE9 (APP/PS1) mouse exhibits normal behavior through age 6 months, and then progressively loses learning and memory (Gimbel et al., 2010; Jankowsky et al., 2003). We considered a role for mGluR5. As reported (Lu et al., 1997; Xu et al., 2009), constitutive mGluR5 deletion impairs performance (Suppl. Fig. S6). Treatment of WT mice with high dose MTEP, 40 mg/kg, impairs alertness and EEG amplitude (Suppl. Fig. S6). Thus, we sought to achieve partial inhibition of mGluR5 with 15 mg/kg MTEP, which does not alter EEG rhythm (Suppl. Fig. S6).

First, we treated WT and APP/PS1 mice with vehicle or MTEP and assessed spatial learning in the radial arm water maze (Fig. 7A). Mice at 9 months age were randomized to blinded treatment with vehicle or MTEP (15 mg/kg, B.I.D. for 10 days) for 3 days prior to, and then for 7 days throughout memory testing. Learning is impaired in transgenics relative to WT, but is fully recovered with MTEP. There is a significant interaction of genotype and drug (two-way repeated-measures (RM) ANOVA: APP/PS1xMTEP interaction, $P<0.01$; APP/PS1, $P<0.01$; MTEP, $P<0.01$).

We extended this finding with alternative memory tests and additional cohorts. Without MTEP treatment, APP/PS1 mice at 9 months age are unable to distinguish novel and familiar objects, whereas WT mice exhibit novel object preference (Fig. 7B; $P<0.001$ for WT). Exploration of two novel objects is not different between genotypes during acclimation (not shown). MTEP-treated APP/PS1 mice recover a novel object preference (Fig. 7B; $P<0.001$ for both WT and APP/PS1 with MTEP).

A separate cohort of APP/PS1 was tested in the Morris water maze. Without treatment, the APP/PS1 mice show greater latencies to locate a hidden platform relative to WT across learning trials (Fig. 7C, RM-ANOVA, $P<0.001$), and spend less time in the target quadrant during a probe trial for memory 24-hours later (Fig. 7D, ANOVA $P<0.001$). In contrast, MTEP-treated APP/PS1 mice are indistinguishable from untreated WT or MTEP-treated WT mice in learning and memory (Fig. 7C, D), but are different from untreated APP/PS1 (Fig. 7C, D; $P<0.001$). There is a significant interaction of genotype and drug (two-way RM-ANOVA in C for APP/PS1xMTEP interaction, $P<0.001$; two-way ANOVA in D, $P<0.001$).

We also administered MTEP to 3XTg mice expressing mutant APP, PS1 and Tau (Oddo et al., 2003). At 8–9 months, these mice perform normally in the Morris water maze (not shown), but are impaired in novel object recognition (Fig. 7E). After randomization to MTEP or vehicle, the 3XTg mice were assessed for novel object recognition (Fig. 7G). MTEP-treated 3XTg mice show a novel object preference ($P<0.01$), but vehicle-treated mice do not. Thus, MTEP reverses memory deficits in two transgenic AD mice.

We considered whether improved memory with MTEP is correlated with a reversal of synaptic loss. A separate cohort of WT and APP/PS1 transgenic mice at 10 months age were treated for 10 days with MTEP, 15 mg/kg B.I.D. As expected, control APP/PS1 mice exhibit a 25–30% decrease in area occupied by presynaptic synaptophysin and postsynaptic PSD-95 immunoreactivity in the dentate gyrus (Fig. 8A–C). The loss of stained synaptic area was

fully rescued by a 10-day course of MTEP (Fig. 8D, E). For WT mice, MTEP did not alter synaptic density. We also assessed synaptic density ultrastructurally, identifying synaptic profiles by the presence of a post-synaptic density and presynaptic vesicles (Fig. 8F). Synapse density in transgenic dentate gyrus increased by 20% with MTEP treatment (Fig. 8G).

DISCUSSION

This study delineates a direct role for mGluR5 in Aβo-related pathophysiology. Of transmembrane PSD proteins, only mGluR5 supports coupling of Aβo–PrP^C to Fyn activation. Intracellular calcium and protein translation are also linked to Aβo–PrP^C engagement via mGluR5. An mGluR5 dependence of signaling is observed for TBS-soluble extracts of AD brain as well as synthetic Aβo, emphasizing the disease relevance. A co-receptor role for mGluR5 is required for dendritic spine loss and transgenic memory impairment. Together, these findings delineate mGluR5 activation as a critical step in Aβo signal transduction with potential for therapeutic intervention.

Dysregulation of mGluR5 signaling in AD

Several previous studies have indirectly implicated mGluR5 in Aβo signaling and in AD. Aβo alters mGluR5 trafficking in neurons, with reduced diffusion, clustering, aberrant activation and neurotoxicity (Renner et al., 2010). The results here provide a PrP^C-based mechanism for these findings and for downstream signaling. Aβo from synthetic, cellular and human AD brain sources suppresses LTP and enhances LTD. These actions are mimicked by mGluR5 agonists and inhibited by mGluR5 antagonists (Rammes et al., 2011; Shankar et al., 2008; Wang et al., 2004). In human AD, mGluR ligand binding is decreased in brain relative to controls and the loss is correlated with disease progression (Albasanz et al., 2005). Proteins titrated by mGluRs, eEF-2, Arc and p70 S6 kinase, are dysregulated in AD brain (An et al., 2003; Li et al., 2005; Wu et al., 2011).

Signaling downstream of mGluR5

Canonical mGluR5 signaling couples to G_q/G_{11} GTPases that activate phospholipase C to produce IP3 and release calcium stores (Luscher and Huber, 2010). mGluR5 also modulates plasma membrane potassium, calcium and TRP channels. Src family tyrosine kinases, including Fyn, have been implicated in linking to NMDA-R (Heidinger et al., 2002; Nicodemo et al., 2010). The proline rich tyrosine kinase 2 (Pyk2) participates in Src/Fyn interaction with mGluR signaling (Heidinger et al., 2002; Nicodemo et al., 2010). The calcium/calmodulin–dependent eEF2 kinase (eEF2K) is bound to mGluR5 in the basal state, but is released during activation to phosphorylate eEF2 (Luscher and Huber, 2010). Phospho-eEF2 reduces global translation, but allows increased Arc/Arg3.1 expression (Park et al., 2008). The Homer family plays a role in mGluR signaling, interacting with receptor and eEF2K (Hu et al., 2010; Luscher and Huber, 2010; Ronesi et al., 2012). Homer interactions with SHANK contribute to PSD localization, specific isoforms have roles in homeostatic scaling.

We show that Aβo–PrP^C complexes leads to several mGluR5 outputs. Fyn activation by Aβo in cortical neurons requires mGluR5 genetically and pharmacologically. Fyn is implicated in Aβo-induced dysregulation of NMDA-R trafficking and activation (Um et al., 2012). Because Fyn binds directly to Tau (Ittner et al., 2010; Lee et al., 2004), this may have implications for AD beyond dysregulation of GluRs.

The Aβo–PrP^C–mGluR5 complex also activates phospholipase C, as detected by monitoring calcium-activated chloride channels in oocytes. The ability of Aβo or human AD brain TBS-

soluble extract to increase calcium in cortical neurons requires mGluR5 and PrP^C. The calcium increase in neurons may occur by the IP3 pathway and also by regulation of NMDA-Rs. Fyn activation by Aβo–PrP^C is as strong as that by Glu, whereas calcium mobilization appears to be an order of magnitude less effective for Aβo PrP^C–than for Glu. Divergence in Aβo–PrP^C–mGluR5 signaling requires further study.

Protein translation plays a major role in mGluR5 signaling (Luscher and Huber, 2010). The phosphorylation of eEF2 is increased by Aβo–PrP^C as much as by mGluR5 agonist. Therefore dysregulation of translation may contribute to synaptic dysfunction in AD. Arc is one protein target of mGluR5 signaling that is up-regulated by Aβo acutely. Calcium and Fyn are independent mediators, which appear to cooperate in eEF2 phosphorylation.

We show that mGluR5 antagonists prevent Aβo-induced spine loss from hippocampal neurons in vitro and in vivo. Critically, MTEP reverses memory deficits in transgenic AD models. Multiple signaling pathways from Aβo–PrP^C–mGluR5 complexes are likely to participate. For spine loss *in vitro*, Fyn is required (Um et al., 2012), but other mGluR5 signaling components may contribute. Protein translation, calcium release and Fyn kinase are each known to participate in plasticity, learning and memory.

Feedback of mGluR5 signaling on Aβ levels

The mGluR5 pathway may also feedback on APP/Aβ metabolism to exacerbate AD. Specifically, mGluR5 agonism elevates Arc, which enhances Aβ production by participating in APP and PS1 co-localization within endocytic vesicles (Wu et al., 2011). Shared pathways between AD and Fragile X have been reported (Sokol et al., 2011). The FRMP protein normally represses APP translation. Transgenic mice with both APP transgenes and loss of FRMP have enhanced phenotypes, including audiogenic seizures, which are treatable with MPEP.

mGluR specificity and localization

Of mGluR receptors, only mGluR1 and mGluR5 interact with Fyn and PrP^C. Only mGluR5 mediates Aβo-induced stimulation of Fyn and calcium signaling in oocytes. *Grm5* gene deletion, and mGluR5-specific compounds reverse Aβo phenotypes, including Fyn activation, neuronal calcium mobilization, eEF2 phosphorylation, spine loss, LDH release and memory deficits. The mGluR1-specific antagonist, MPMQ, does not block. Thus, mGluR5 appears to be specifically involved in Aβo–PrP^C action.

PrP^C, mGluR5 and Fyn have all been localized to the PSD by subcellular fractionation. For PrP^C and Fyn, high-resolution *in situ* protein localization in brain has not been reported. For mGluR5, imaging confirms a post-synaptic localization and indicates that mGluR5 is dynamically located at the PSD periphery (Lujan et al., 1996). Dynamic regulation of mGluR5 localization by Aβo has been observed (Renner et al., 2010).

Short term activation *versus* longer term desensitization

While ionotropic receptors function rapidly, metabotropic receptors are slow and show prominent desensitization. Aβo levels are highly unlikely to fluctuate on the time scale of synaptic transmission, so Aβo–PrP^C complexes may engage mGluR5 and elicit a degree of desensitization that prevents responsiveness to cyclic changes in Glu. Thus, mGluR5 may be dysregulated by acute activation and chronic desensitization.

Alternate ligands and accessory ectodomains for mGluRs

Activation of mGluR5 by Aβo–PrP^C complexes expands the repertoire of metabotropic glutamate receptors. Certain other G protein coupled receptors (GPCRs) respond to more

than one ligand, and interact extracellularly with accessory subunits or co-receptors. Melanocortin receptors recognize both melanocortin agonists and Agouti/AgRP antagonists with specificity modified by MRAPs (Breit et al., 2011). Calcitonin and related receptors have ligand preference altered by transmembrane RAMPs (Hay et al., 2006). Non-canonical signaling by Hedgehogs and Wnts through Smoothened and Frizzleds to heterotrimeric G proteins depends on ligand interaction with Patched and LRP5/6, respectively (Angers and Moon, 2009; Robbins et al., 2012). Ectodomain accessory proteins for mGluRs have not been recognized previously, so PrP^C is unique. The only previously known endogenous ligand for mGluR5 is Glu, so the action of Aβo–PrP^C is novel. Our findings raise the possibility that mGluR5 may be regulated physiologically by molecules other than Glu.

Targeting mGluR5 for AD therapy

The delineation of an Aβo–PrP^C–mGluR5–Fyn pathway provides potential targets for AD intervention. Antibodies that block Aβo binding to PrP^C reverse memory deficits in transgenic AD mice (Chung et al., 2010) and we show that a mGluR5 negative allosteric modulator has a similar effect. However, full mGluR5 antagonism may have deleterious effects on neuronal function and impairment of baseline attention (Luscher and Huber, 2010; Simonyi et al., 2010). Deficits of contextual fear conditioning and inhibitory learning are observed in the absence of mGluR5 (Xu et al., 2009), and mGluR5 function may contribute to healthy brain aging (Lee et al., 2005; Menard and Quirion, 2012; Nicolle et al., 1999). Optimal intervention may therefore be designed to prevent Aβo–PrP^C activation of mGluR5, without modifying Glu activation of mGluR5.

EXPERIMENTAL PROCEDURES

Mouse strains

The mouse strains have been described previously (Gimbel et al., 2010; Jankowsky et al., 2003; Lu et al., 1997; Oddo et al., 2003).

Cell Culture and Biochemistry

Standard procedures were utilized, including the assessment of intracellular calcium level in neuronal culture (Um et al., 2012) and voltage clamp recording from *X. laevis* oocytes (Lauren et al., 2009; Strittmatter et al., 1993). Fresh-frozen post-mortem human pre-frontal cortex from the brains of AD patients were obtained, as approved by Institutional Review Board collected at NYU and at Yale. Particulate components were removed from TBS homogenates by centrifugation at 100,000 x *g* for 30 minutes.

MTEP treatment and memory testing of transgenic mice

Mice were randomized to treatment groups and the experimenter was unaware of treatment status throughout behavioral testing. Procedures for Morris water maze testing have been described (Gimbel et al., 2010).

Extended Experimental Procedures are available in the online supplement.

Supplementary Material

Refer to Web version on PubMed Central for supplementary material.

Acknowledgments

We thank Yiguang Fu and Stefano Sodi for excellent technical support. We thank Xinran Liu of the Yale Center for Cell Imaging for advice on synapse ultrastructure analysis. S.M.S. is a co-founder of Axerion Therapeutics, seeking

to develop NgR- and PrP-based therapeutics. H.B.N. is an Ellison Medical Foundation AFAR Postdoctoral Fellow and S.M.S. is a member of the Kavli Institute for Neuroscience at Yale University. We acknowledge support from the National Institutes of Health to S.M.S., A.J.K. and T. W., and from the Falk Medical Research Trust and the Alzheimer's Association to S.M.S.

References

Abu-Elneel K, Ochiishi T, Medina M, Remedi M, Gastaldi L, Caceres A, Kosik KS. A delta-catenin signaling pathway leading to dendritic protrusions. J Biol Chem. 2008; 283:32781–32791. [PubMed: 18809680]

Albasanz JL, Dalfo E, Ferrer I, Martin M. Impaired metabotropic glutamate receptor/phospholipase C signaling pathway in the cerebral cortex in Alzheimer's disease and dementia with Lewy bodies correlates with stage of Alzheimer's-disease-related changes. Neurobiology of disease. 2005; 20:685–693. [PubMed: 15949941]

An WL, Cowburn RF, Li L, Braak H, Alafuzoff I, Iqbal K, Iqbal IG, Winblad B, Pei JJ. Up-regulation of phosphorylated/activated p70 S6 kinase and its relationship to neurofibrillary pathology in Alzheimer's disease. Am J Pathol. 2003; 163:591–607. [PubMed: 12875979]

Angers S, Moon RT. Proximal events in Wnt signal transduction. Nat Rev Mol Cell Biol. 2009; 10:468–477. [PubMed: 19536106]

Bai Y, Markham K, Chen F, Weerasekera R, Watts J, Horne P, Wakutani Y, Bagshaw R, Mathews PM, Fraser PE, et al. The in vivo brain interactome of the amyloid precursor protein. Mol Cell Proteomics. 2008; 7:15–34. [PubMed: 17934213]

Barry AE, Klyubin I, Mc Donald JM, Mably AJ, Farrell MA, Scott M, Walsh DM, Rowan MJ. Alzheimer's disease brain-derived amyloid-beta-mediated inhibition of LTP in vivo is prevented by immunotargeting cellular prion protein. J Neurosci. 2011; 31:7259–7263. [PubMed: 21593310]

Bizat N, Peyrin JM, Haik S, Cochois V, Beaudry P, Laplanche JL, Neri C. Neuron dysfunction is induced by prion protein with an insertional mutation via a Fyn kinase and reversed by sirtuin activation in Caenorhabditis elegans. J Neurosci. 2010; 30:5394–5403. [PubMed: 20392961]

Breit A, Buch TR, Boekhoff I, Solinski HJ, Damm E, Gudermann T. Alternative G protein coupling and biased agonism: new insights into melanocortin-4 receptor signalling. Mol Cell Endocrinol. 2011; 331:232–240. [PubMed: 20674667]

Chen S, Yadav SP, Surewicz WK. Interaction between human prion protein and amyloid-beta (Abeta) oligomers: role OF N-terminal residues. J Biol Chem. 2010; 285:26377–26383. [PubMed: 20576610]

Choi KY, Chung S, Roche KW. Differential binding of calmodulin to group I metabotropic glutamate receptors regulates receptor trafficking and signaling. J Neurosci. 2011; 31:5921–5930. [PubMed: 21508217]

Chung E, Ji Y, Sun Y, Kascsak RJ, Kascsak RB, Mehta PD, Strittmatter SM, Wisniewski T. Anti-PrPC monoclonal antibody infusion as a novel treatment for cognitive deficits in an alzheimer's disease model mouse. BMC Neurosci. 2010; 11:130. [PubMed: 20946660]

Cisse M, Halabisky B, Harris J, Devidze N, Dubal DB, Sun B, Orr A, Lotz G, Kim DH, Hamto P, et al. Reversing EphB2 depletion rescues cognitive functions in Alzheimer model. Nature. 2011; 469:47–52. [PubMed: 21113149]

Collins MO, Husi H, Yu L, Brandon JM, Anderson CN, Blackstock WP, Choudhary JS, Grant SG. Molecular characterization and comparison of the components and multiprotein complexes in the postsynaptic proteome. Journal of neurochemistry. 2006; 97(Suppl 1):16–23. [PubMed: 16635246]

Dravid SM, Murray TF. Spontaneous synchronized calcium oscillations in neocortical neurons in the presence of physiological [Mg(2+)]: involvement of AMPA/kainate and metabotropic glutamate receptors. Brain Res. 2004; 1006:8–17. [PubMed: 15047019]

Emes RD, Pocklington AJ, Anderson CN, Bayes A, Collins MO, Vickers CA, Croning MD, Malik BR, Choudhary JS, Armstrong JD, Grant SG. Evolutionary expansion and anatomical specialization of synapse proteome complexity. Nat Neurosci. 2008; 11:799–806. [PubMed: 18536710]

Freir DB, Nicoll AJ, Klyubin I, Panico S, Mc Donald JM, Risse E, Asante EA, Farrow MA, Sessions RB, Saibil HR, et al. Interaction between prion protein and toxic amyloid beta assemblies can be therapeutically targeted at multiple sites. Nat Commun. 2011; 2:336. [PubMed: 21654636]

Gimbel DA, Nygaard HB, Coffey EE, Gunther EC, Lauren J, Gimbel ZA, Strittmatter SM. Memory impairment in transgenic Alzheimer mice requires cellular prion protein. J Neurosci. 2010; 30:6367–6374. [PubMed: 20445063]

Grant SG, O'Dell TJ, Karl KA, Stein PL, Soriano P, Kandel ER. Impaired long-term potentiation, spatial learning, and hippocampal development in fyn mutant mice. Science. 1992; 258:1903–1910. [PubMed: 1361685]

Hay DL, Poyner DR, Sexton PM. GPCR modulation by RAMPs. Pharmacol Ther. 2006; 109:173–197. [PubMed: 16111761]

Heidinger V, Manzerra P, Wang XQ, Strasser U, Yu SP, Choi DW, Behrens MM. Metabotropic glutamate receptor 1-induced upregulation of NMDA receptor current: mediation through the Pyk2/Src-family kinase pathway in cortical neurons. J Neurosci. 2002; 22:5452–5461. [PubMed: 12097497]

Holtzman DM, Morris JC, Goate AM. Alzheimer's disease: the challenge of the second century. Science translational medicine. 2011; 3:77sr71.

Hu JH, Park JM, Park S, Xiao B, Dehoff MH, Kim S, Hayashi T, Schwarz MK, Huganir RL, Seeburg PH, et al. Homeostatic scaling requires group I mGluR activation mediated by Homer1a. Neuron. 2010; 68:1128–1142. [PubMed: 21172614]

Ittner LM, Ke YD, Delerue F, Bi M, Gladbach A, van Eersel J, Wolfing H, Chieng BC, Christie MJ, Napier IA, et al. Dendritic function of tau mediates amyloid-beta toxicity in Alzheimer's disease mouse models. Cell. 2010; 142:387–397. [PubMed: 20655099]

Jankowsky JL, Xu G, Fromholt D, Gonzales V, Borchelt DR. Environmental enrichment exacerbates amyloid plaque formation in a transgenic mouse model of Alzheimer disease. J Neuropathol Exp Neurol. 2003; 62:1220–1227. [PubMed: 14692698]

Jonsson T, Atwal JK, Steinberg S, Snaedal J, Jonsson PV, Bjornsson S, Stefansson H, Sulem P, Gudbjartsson D, Maloney J, et al. A mutation in APP protects against Alzheimer's disease and age-related cognitive decline. Nature. 2012; 488:96–99. [PubMed: 22801501]

Larson M, Sherman MA, Amar F, Nuvolone M, Schneider JA, Bennett DA, Aguzzi A, Lesne SE. The Complex PrPc-Fyn Couples Human Oligomeric Abeta with Pathological Tau Changes in Alzheimer's Disease. J Neurosci. 2012; 32:16857–16871. [PubMed: 23175838]

Lauren J, Gimbel DA, Nygaard HB, Gilbert JW, Strittmatter SM. Cellular prion protein mediates impairment of synaptic plasticity by amyloid-beta oligomers. Nature. 2009; 457:1128–1132. [PubMed: 19242475]

Lee G, Thangavel R, Sharma VM, Litersky JM, Bhaskar K, Fang SM, Do LH, Andreadis A, Van Hoesen G, Ksiezak-Reding H. Phosphorylation of tau by fyn: implications for Alzheimer's disease. J Neurosci. 2004; 24:2304–2312. [PubMed: 14999081]

Lee HK, Min SS, Gallagher M, Kirkwood A. NMDA receptor-independent long-term depression correlates with successful aging in rats. Nat Neurosci. 2005; 8:1657–1659. [PubMed: 16286930]

Li X, Alafuzoff I, Soininen H, Winblad B, Pei JJ. Levels of mTOR and its downstream targets 4E-BP1, eEF2, and eEF2 kinase in relationships with tau in Alzheimer's disease brain. The FEBS journal. 2005; 272:4211–4220. [PubMed: 16098202]

Linhoff MW, Lauren J, Cassidy RM, Dobie FA, Takahashi H, Nygaard HB, Airaksinen MS, Strittmatter SM, Craig AM. An unbiased expression screen for synaptogenic proteins identifies the LRRTM protein family as synaptic organizers. Neuron. 2009; 61:734–749. [PubMed: 19285470]

Lu YM, Jia Z, Janus C, Henderson JT, Gerlai R, Wojtowicz JM, Roder JC. Mice lacking metabotropic glutamate receptor 5 show impaired learning and reduced CA1 long-term potentiation (LTP) but normal CA3 LTP. J Neurosci. 1997; 17:5196–5205. [PubMed: 9185557]

Lujan R, Nusser Z, Roberts JD, Shigemoto R, Somogyi P. Perisynaptic location of metabotropic glutamate receptors mGluR1 and mGluR5 on dendrites and dendritic spines in the rat hippocampus. Eur J Neurosci. 1996; 8:1488–1500. [PubMed: 8758956]

Luscher C, Huber KM. Group 1 mGluR-dependent synaptic long-term depression: mechanisms and implications for circuitry and disease. Neuron. 2010; 65:445–459. [PubMed: 20188650]

Majercak J, Ray WJ, Espeseth A, Simon A, Shi XP, Wolffe C, Getty K, Marine S, Stec E, Ferrer M, et al. LRRTM3 promotes processing of amyloid-precursor protein by BACE1 and is a positional candidate gene for late-onset Alzheimer's disease. Proc Natl Acad Sci U S A. 2006; 103:17967–17972. [PubMed: 17098871]

Malaga-Trillo E, Solis GP, Schrock Y, Geiss C, Luncz L, Thomanetz V, Stuermer CA. Regulation of embryonic cell adhesion by the prion protein. PLoS Biol. 2009; 7:e55. [PubMed: 19278297]

Menard C, Quirion R. Successful cognitive aging in rats: a role for mGluR5 glutamate receptors, homer 1 proteins and downstream signaling pathways. PLoS ONE. 2012; 7:e28666. [PubMed: 22238580]

Moult PR, Gladding CM, Sanderson TM, Fitzjohn SM, Bashir ZI, Molnar E, Collingridge GL. Tyrosine phosphatases regulate AMPA receptor trafficking during metabotropic glutamate receptor-mediated long-term depression. J Neurosci. 2006; 26:2544–2554. [PubMed: 16510732]

Nicodemo AA, Pampillo M, Ferreira LT, Dale LB, Cregan T, Ribeiro FM, Ferguson SS. Pyk2 uncouples metabotropic glutamate receptor G protein signaling but facilitates ERK1/2 activation. Mol Brain. 2010; 3:4. [PubMed: 20180987]

Nicolle MM, Colombo PJ, Gallagher M, McKinney M. Metabotropic glutamate receptor-mediated hippocampal phosphoinositide turnover is blunted in spatial learning-impaired aged rats. J Neurosci. 1999; 19:9604–9610. [PubMed: 10531462]

Oddo S, Caccamo A, Shepherd JD, Murphy MP, Golde TE, Kayed R, Metherate R, Mattson MP, Akbari Y, LaFerla FM. Triple-transgenic model of Alzheimer's disease with plaques and tangles: intracellular Abeta and synaptic dysfunction. Neuron. 2003; 39:409–421. [PubMed: 12895417]

Park S, Park JM, Kim S, Kim JA, Shepherd JD, Smith-Hicks CL, Chowdhury S, Kaufmann W, Kuhl D, Ryazanov AG, et al. Elongation factor 2 and fragile X mental retardation protein control the dynamic translation of Arc/Arg3.1 essential for mGluR-LTD. Neuron. 2008; 59:70–83. [PubMed: 18614030]

Prybylowski K, Chang K, Sans N, Kan L, Vicini S, Wenthold RJ. The synaptic localization of NR2B-containing NMDA receptors is controlled by interactions with PDZ proteins and AP-2. Neuron. 2005; 47:845–857. [PubMed: 16157279]

Rammes G, Hasenjager A, Sroka-Saidi K, Deussing JM, Parsons CG. Therapeutic significance of NR2B-containing NMDA receptors and mGluR5 metabotropic glutamate receptors in mediating the synaptotoxic effects of beta-amyloid oligomers on long-term potentiation (LTP) in murine hippocampal slices. Neuropharmacology. 2011; 60:982–990. [PubMed: 21310164]

Renner M, Lacor PN, Velasco PT, Xu J, Contractor A, Klein WL, Triller A. Deleterious effects of amyloid beta oligomers acting as an extracellular scaffold for mGluR5. Neuron. 2010; 66:739–754. [PubMed: 20547131]

Robbins DJ, Fei DL, Riobo NA. The Hedgehog signal transduction network. Sci Signal. 2012; 5:re6. [PubMed: 23074268]

Roberson ED, Halabisky B, Yoo JW, Yao J, Chin J, Yan F, Wu T, Hamto P, Devidze N, Yu GQ, et al. Amyloid-beta/Fyn-induced synaptic, network, and cognitive impairments depend on tau levels in multiple mouse models of Alzheimer's disease. J Neurosci. 2011; 31:700–711. [PubMed: 21228179]

Ronesi JA, Collins KA, Hays SA, Tsai NP, Guo W, Birnbaum SG, Hu JH, Worley PF, Gibson JR, Huber KM. Disrupted Homer scaffolds mediate abnormal mGluR5 function in a mouse model of fragile X syndrome. Nat Neurosci. 2012; 15:431–440. S431. [PubMed: 22267161]

Saugstad JA, Segerson TP, Westbrook GL. Metabotropic glutamate receptors activate G-protein-coupled inwardly rectifying potassium channels in Xenopus oocytes. J Neurosci. 1996; 16:5979–5985. [PubMed: 8815880]

Schmitt-Ulms G, Hansen K, Liu J, Cowdrey C, Yang J, DeArmond SJ, Cohen FE, Prusiner SB, Baldwin MA. Time-controlled transcardiac perfusion cross-linking for the study of protein interactions in complex tissues. Nature biotechnology. 2004; 22:724–731.

Shankar GM, Li S, Mehta TH, Garcia-Munoz A, Shepardson NE, Smith I, Brett FM, Farrell MA, Rowan MJ, Lemere CA, et al. Amyloid-beta protein dimers isolated directly from Alzheimer's brains impair synaptic plasticity and memory. Nat Med. 2008; 14:837–842. [PubMed: 18568035]

Shinoda Y, Tanaka T, Tominaga-Yoshino K, Ogura A. Persistent synapse loss induced by repetitive LTD in developing rat hippocampal neurons. PLoS ONE. 2010; 5:e10390. [PubMed: 20436928]

Simonyi A, Schachtman TR, Christoffersen GR. Metabotropic glutamate receptor subtype 5 antagonism in learning and memory. European journal of pharmacology. 2010; 639:17–25. [PubMed: 20363219]

Sokol DK, Maloney B, Long JM, Ray B, Lahiri DK. Autism, Alzheimer disease, and fragile X: APP, FMRP, and mGluR5 are molecular links. Neurology. 2011; 76:1344–1352. [PubMed: 21482951]

Strittmatter SM, Cannon SC, Ross EM, Higashijima T, Fishman MC. GAP-43 augments G protein-coupled receptor transduction in Xenopus laevis oocytes. Proc Natl Acad Sci U S A. 1993; 90:5327–5331. [PubMed: 7685122]

Takasu MA, Dalva MB, Zigmond RE, Greenberg ME. Modulation of NMDA receptor-dependent calcium influx and gene expression through EphB receptors. Science. 2002; 295:491–495. [PubMed: 11799243]

Um JW, Nygaard HB, Heiss JK, Kostylev MA, Stagi M, Vortmeyer A, Wisniewski T, Gunther EC, Strittmatter SM. Alzheimer amyloid-beta oligomer bound to postsynaptic prion protein activates Fyn to impair neurons. Nat Neurosci. 2012; 15:1227–1235. [PubMed: 22820466]

Um JW, Strittmatter SM. Amyloid-beta induced signaling by cellular prion protein and Fyn kinase in Alzheimer disease. Prion. 2013; 7:37–41. [PubMed: 22987042]

Vanderklish PW, Edelman GM. Dendritic spines elongate after stimulation of group 1 metabotropic glutamate receptors in cultured hippocampal neurons. Proc Natl Acad Sci U S A. 2002; 99:1639–1644. [PubMed: 11818568]

Wang Q, Walsh DM, Rowan MJ, Selkoe DJ, Anwyl R. Block of long-term potentiation by naturally secreted and synthetic amyloid beta-peptide in hippocampal slices is mediated via activation of the kinases c-Jun N-terminal kinase, cyclin-dependent kinase 5, and p38 mitogen-activated protein kinase as well as metabotropic glutamate receptor type 5. J Neurosci. 2004; 24:3370–3378. [PubMed: 15056716]

Wu J, Petralia RS, Kurushima H, Patel H, Jung MY, Volk L, Chowdhury S, Shepherd JD, Dehoff M, Li Y, et al. Arc/Arg3.1 regulates an endosomal pathway essential for activity-dependent beta-amyloid generation. Cell. 2011; 147:615–628. [PubMed: 22036569]

Xu J, Zhu Y, Contractor A, Heinemann SF. mGluR5 has a critical role in inhibitory learning. J Neurosci. 2009; 29:3676–3684. [PubMed: 19321764]

Zou WQ, Xiao X, Yuan J, Puoti G, Fujioka H, Wang X, Richardson S, Zhou X, Zou R, Li S, et al. Amyloid-{beta}42 Interacts Mainly with Insoluble Prion Protein in the Alzheimer Brain. J Biol Chem. 2011; 286:15095–15105. [PubMed: 21393248]

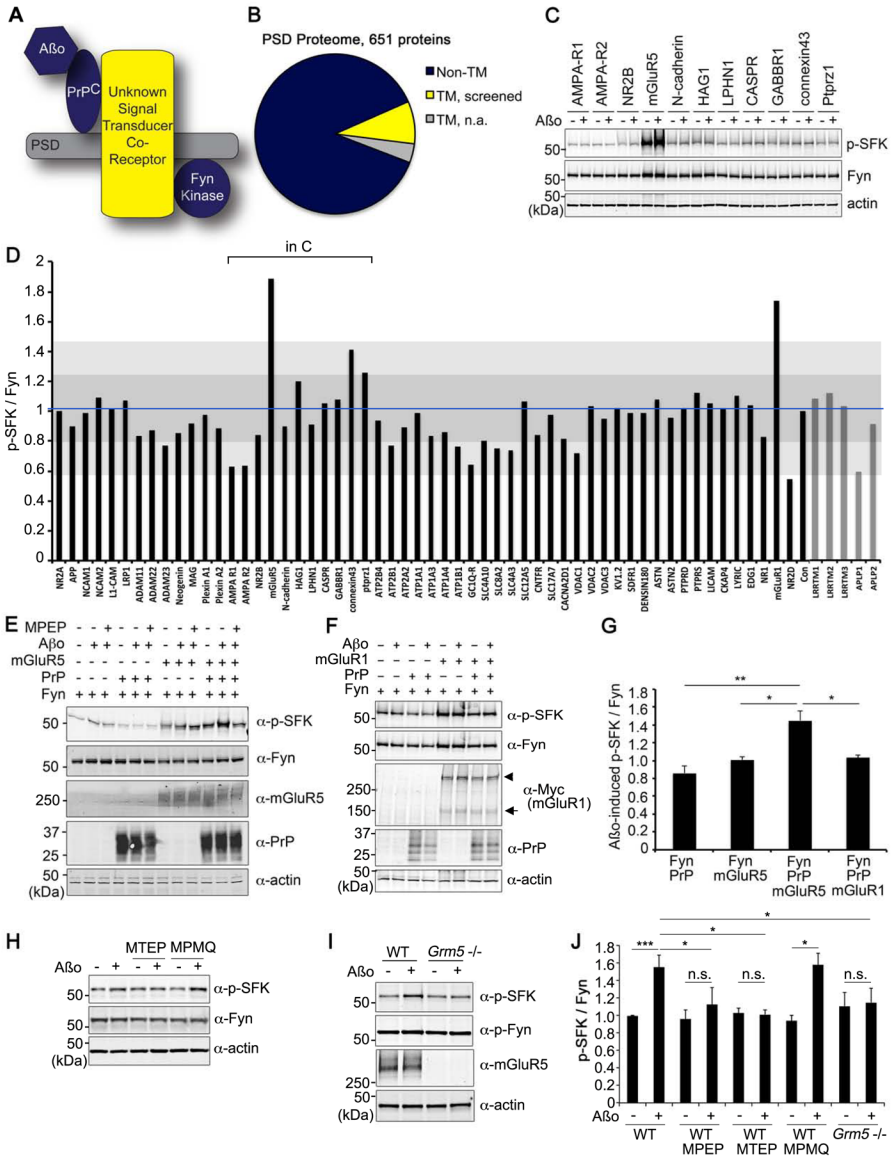

Figure 1. Metabotropic GluR5 Links Aβo/PrP^C Complexes to Fyn

A Schematic indicating that Aβo/PrP^C complexes require a co-receptor to activate Fyn in PSDs.

B Pie charts show transmembrane proteins (81) among total PSD proteins (651). Transmembrane proteins were subdivided; those that were screened in Aβo/Fyn assays (56, yellow) and those not (25, gray).

C Immunoblot of screening for Fyn activation. HEK293T cells were transfected with expression vectors for Fyn, PrP^C or candidate genes. After treatment with 1 μM Aβo for 15 min, lysates were analyzed by anti-phospho-SFK (Tyr 416) or anti-Fyn immunoblot.

D The ratio of phospho-SFK to Fyn is plotted from 3 experiments with Aβo. Blue line indicates the mean of all controls. Dark gray is one standard deviation, and light gray is two standard deviations from control.

E HEK293T cells were transfected with vectors for Fyn, PrP^C or mGluR5, and treated with 0 or 1 μM Aβo for 15 min. Some cultures were pre-incubated for 30 min with 100 μM

MPEP prior to Aβ. Lysates were analyzed by anti-phospho-SFK (Tyr 416), anti-Fyn, anti-mGluR5, or anti-PrP^C immunoblot. Actin is loading control.

F HEK293T cells were transfected with vectors for Fyn, PrP^C or Myc-mGluR1 as indicated. After cell treatment with 0 or 1 μM Aβo for 15 min, lysates were analyzed by anti-phospho-SFK (Tyr 416), anti-Fyn, anti-Myc, or anti-PrP^C immunoblot. Actin is loading control.

G Quantification of phospho-SFK level in lysates from E, F, normalized to Fyn. Mean±sem, n=4 experiments. **, $P<0.01$; *, $P<0.05$; ANOVA, Tukey post-hoc pairwise comparisons.

H Cortical neurons from E17 WT mice at 21 DIV were treated with 0 or 1 μM of Aβo for 15 min. Indicated samples were treated with 100 μM MTEP or 10 μM MPMQ for 30 min prior to Aβo. Lysates were subjected to immunoblot with anti-Fyn, or anti-phospho-SFK (Tyr 416). Actin is loading control.

I Cortical neurons from WT or *Grm5*−/− mice after 21 DIV were treated with 0 or 1 μM Aβo for 15 min. Lysates were analyzed by anti-phospho-SFK (Tyr 416), anti-Fyn, anti-mGluR5 immunoblot. Actin is loading control.

J Quantification of phospho-SFK level in lysates from H, I, normalized to Fyn. Mean±sem, n=3 experiments. ***, $P<0.001$; *, $P<0.05$; ANOVA, Tukey post-hoc pairwise comparisons. See also Fig. S1.

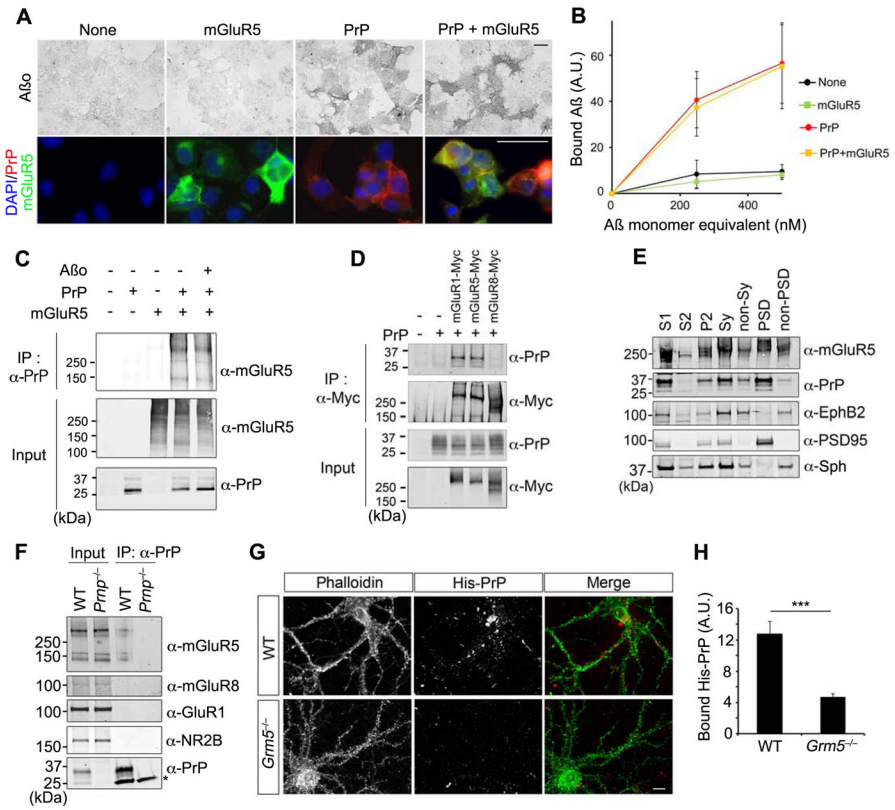

Figure 2. PrP^{C} Interacts with mGluR5

A Aβo (250 nM) binding to COS7 cells expressing mGluR5, PrP^{C}, or co-expressing mGluR5 with PrP^{C} (upper). Protein expression was confirmed by immunofluorescence (bottom). Scale bar, 50 μm.

B Dose-response for Aβo binding to COS7 cells from experiments as in A. Mean±sem, n=3 experiments.

C HEK293T cells were transfected with vector for either mGluR5 or PrP^{C}, or co-transfected for mGluR5 and PrP^{C}. After treatment with 0 or 1 μM Aβo for 1 h, lysates (input) and anti-PrP^{C} immunoprecipitates were immunoblotted with either anti-mGluR5 or anti-PrP^{C}.

D HEK293T cells were transfected with vector for PrP^{C} or co-transfected with different Myc-tagged mGluRs and PrP^{C}, as indicated. Lysates (input) and anti-Myc immunoprecipitates were immunoblotted with either anti-Myc or anti-PrP^{C} antibodies.

E Indicated fractions (20 μg protein) were prepared and analyzed by immunoblot with anti-PrP^{C}, anti-mGluR5, anti-EphB2, anti-PSD95, anti-synaptophysin, and anti-actin antibodies.

F Brain lysates from WT or *Prnp* −/− mice were cross-linked with the cleavable DTSSP. Whole lysates (5% Input) and anti-PrP^{C} immunoprecipitates were immunoblotted with anti-mGluR5, anti-mGluR8, anti-NR2B, anti-GluR1 or anti-PrP antibodies. Asterisk, Ig light chain.

G His-tagged human PrP^{C} was incubated with DIV21 WT or *Grm5* −/− neurons for 1 h. Neurons were then fixed and stained with human-specific anti-PrP^{C} antibody and Alexa-568 secondary antibody with rhodamine-phalloidin as counterstain. Scale bar, 10 μm.

H Quantification of His-PrP^{C} bound to WT or *Grm5* −/− neurons. His-PrP^{C} immunofluorescence was measured by ImageJ in segments of primary dendrites 10 μm from the soma and background-subtracted. Mean±sem, n=3 embryos for each genotype.***, $P<0.001$; Student's two-tailed *t* test.

See also Fig. S2.

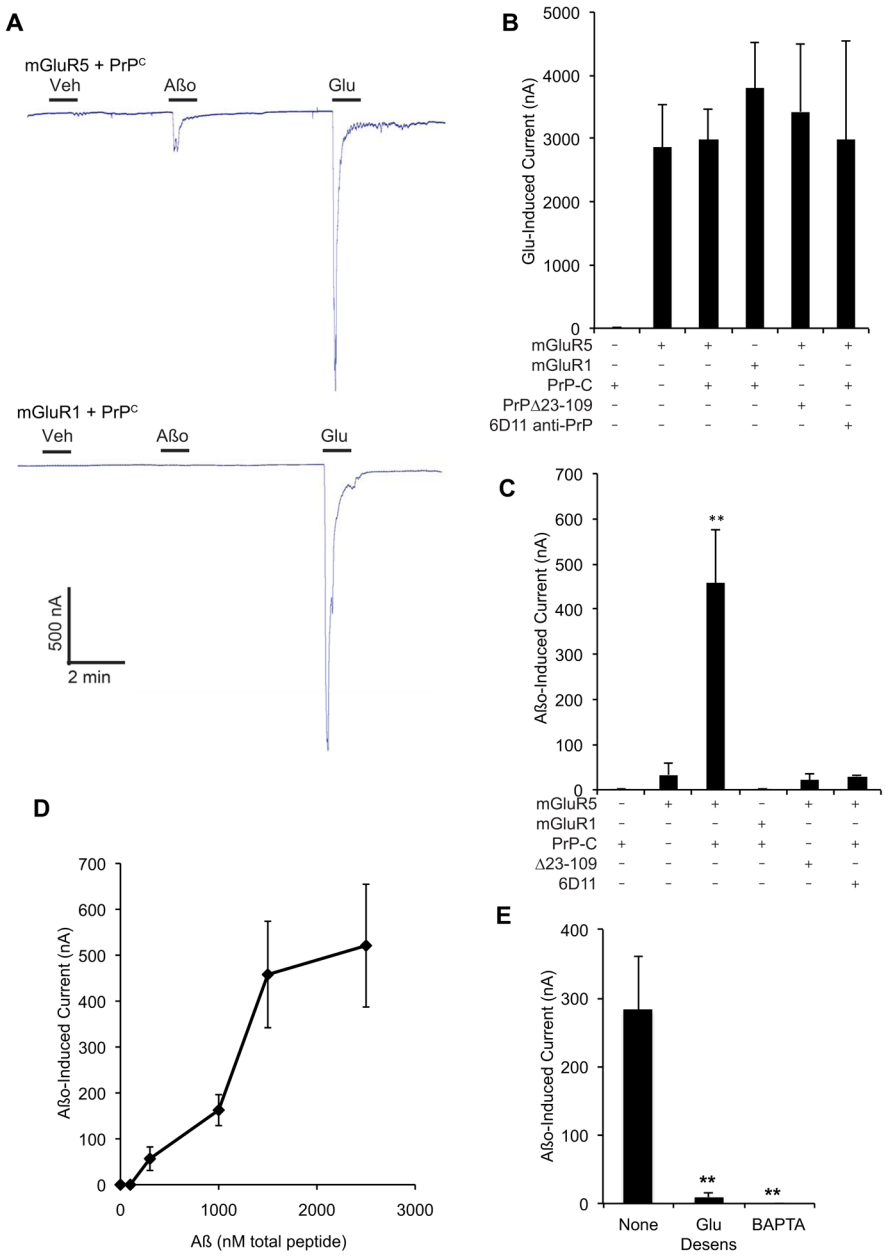

Figure 3. Aβo directly stimulate mGluR5

A Representative traces obtained from oocytes expressing mGluR5 plus PrP^C, or mGluR1 plus PrP^C. Bath application (bars) of Aβo (1.5 μM monomer equivalent, estimated 15 nM oligomer) or Glu (100 μM) elicits an inward current from mGluR5 plus PrP^C oocyte. Exposure to Glu, but not Aβo, elicits a response in oocytes expressing mGluR1 and PrP^C.

B, C Quantification of the peak current elicited by glutamate (B) or Aβo (C) in oocytes expressing the indicated proteins, with or without pre-treatment with 5 μg/ml anti-PrP^C antibody, 6D11. Data are Mean±sem, n=8–28 oocytes. **, $P<0.01$; ANOVA, Tukey post-hoc pairwise comparisons.

D Dose response for Aβo-induced current in oocytes expressing mGluR5 and PrP^C. Mean ±sem for n = 4–7 oocytes.

E Oocytes expressing mGluR5 and PrP^C were either treated for 1 min with 100 μM Glu to maximally stimulate a response 3 min prior to testing for an Aβo response, or not pre-stimulated with Glu. Alternatively, some oocytes were preincubated with 100 μM BAPTA-AM for 60 minutes. After these pretreatments, the peak inward current was measured in response to 1.5 μM Aβo. Mean±sem, n=6–12 oocytes. **, $P<0.005$; ANOVA, Tukey post-hoc pairwise comparisons.
See also Fig. S4.

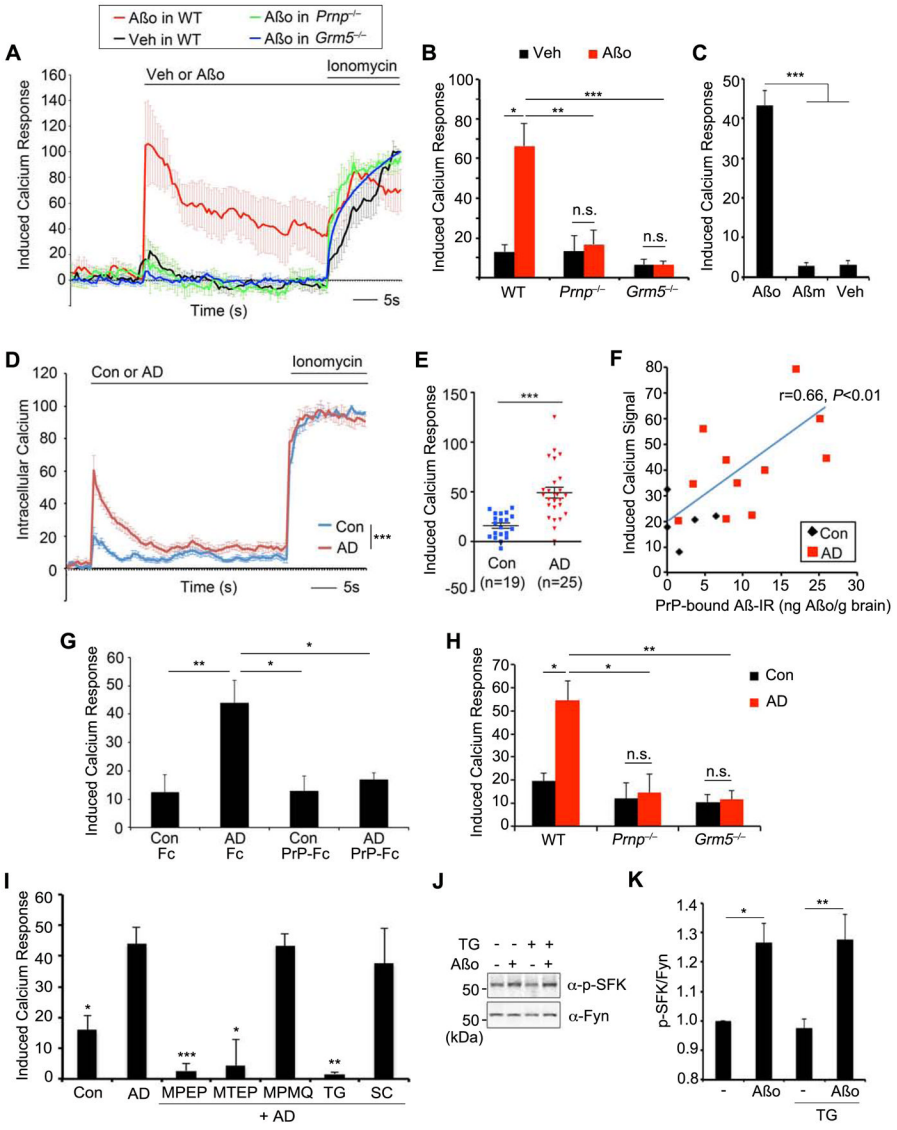

Figure 4. Aβ species from human AD brains or synthetic Aβo increase intracellular calcium via PrP and mGluR5

A Change of intracellular calcium in E17 cortical neurons from WT, *Prnp* −/− or *Grm5* −/− mice in response to Aβo, vehicle (Veh) or ionomycin (500 nM) was monitored by FLIPR calcium assay. Mean±sem, n=24–40 wells from 3–5 embryos per genotype.

B Quantification of calcium response induced by Aβo or vehicle (Veh) from A. *, $P<0.05$, **, $P<0.01$ ***, $P<0.001$; ANOVA, Tukey post-hoc pairwise comparisons.

C Quantification of calcium response induced by oligomeric Aβ (Aβo), monomeric Aβ (Aβm) or vehicle (Veh). ***, $P<0.001$; ANOVA, Tukey post-hoc pairwise comparisons.

D Intracellular calcium in E17 cortical neurons in response to human AD brain extracts (AD), n=25, age-matched control brain (Con), n=19 (1.5 μg total protein/ml) or ionomycin (500 nM) monitored by FLIPR calcium assay. Mean±sem, ***, $P<0.001$ by Repeated Measures ANOVA for 10 seconds window after AD brain extract.

E Quantification of calcium response induced by AD or Con extracts from C. Each dot is from a different brain. ***, $P<0.001$ by Student's two-tailed *t* test.

F Correlation between AD extract-induced calcium and PrP(23-111)-interacting Aβ species is plotted. Each point is from a different brain sample. Pearson coefficient of linear correlation reported with two-tailed *P*.

G Calcium response induced by AD extracts preabsorbed with Fc (AD Fc) or PrP^{C}-Fc resin (AD PrP-Fc), or Con extracts preabsorbed with Fc (Con Fc) or PrP^{C}-Fc resin (Con PrP-Fc). *, $P<0.05$, **, $P<0.01$; ANOVA, Tukey post-hoc pairwise comparisons.

H Calcium response induced by AD or Con extracts in E17 cortical neurons from WT, *Prnp* $-/-$ or *Grm5* $-/-$ mice. Mean±sem, n = 3 independent embryos for each genotype. *, $P<0.05$, **, $P<0.01$; ANOVA, Tukey post-hoc comparisons.

I Calcium response induced by AD or Con extracts in WT cortical neurons. Neurons were pretreated with 100 μM MPEP, 100 μM MTEP, 10 μM MPMQ, 500 nM saracatinib for 1 h or 100 nM thapsigargin for 24 h prior to AD extract. *, $P<0.05$, **, $P<0.01$, ***, $P<0.001$; ANOVA, Tukey post-hoc pairwise comparisons to AD extract only samples.

J WT cortical neurons were treated with 0 or 1 μM Aβo for 15 min. Indicated sample was treated with 100 nM thapsigargin for 24 h prior to Aβo. Lysates were analyzed by anti-phospho-SFK or anti-Fyn immunoblot.

K Quantification of phospho-SFK level in the lysate normalized to Fyn from 3 experiments. Mean±sem, *, $P<0.05$; **, $P<0.01$; ANOVA, Tukey post-hoc pairwise comparisons.

See also Fig. S3.

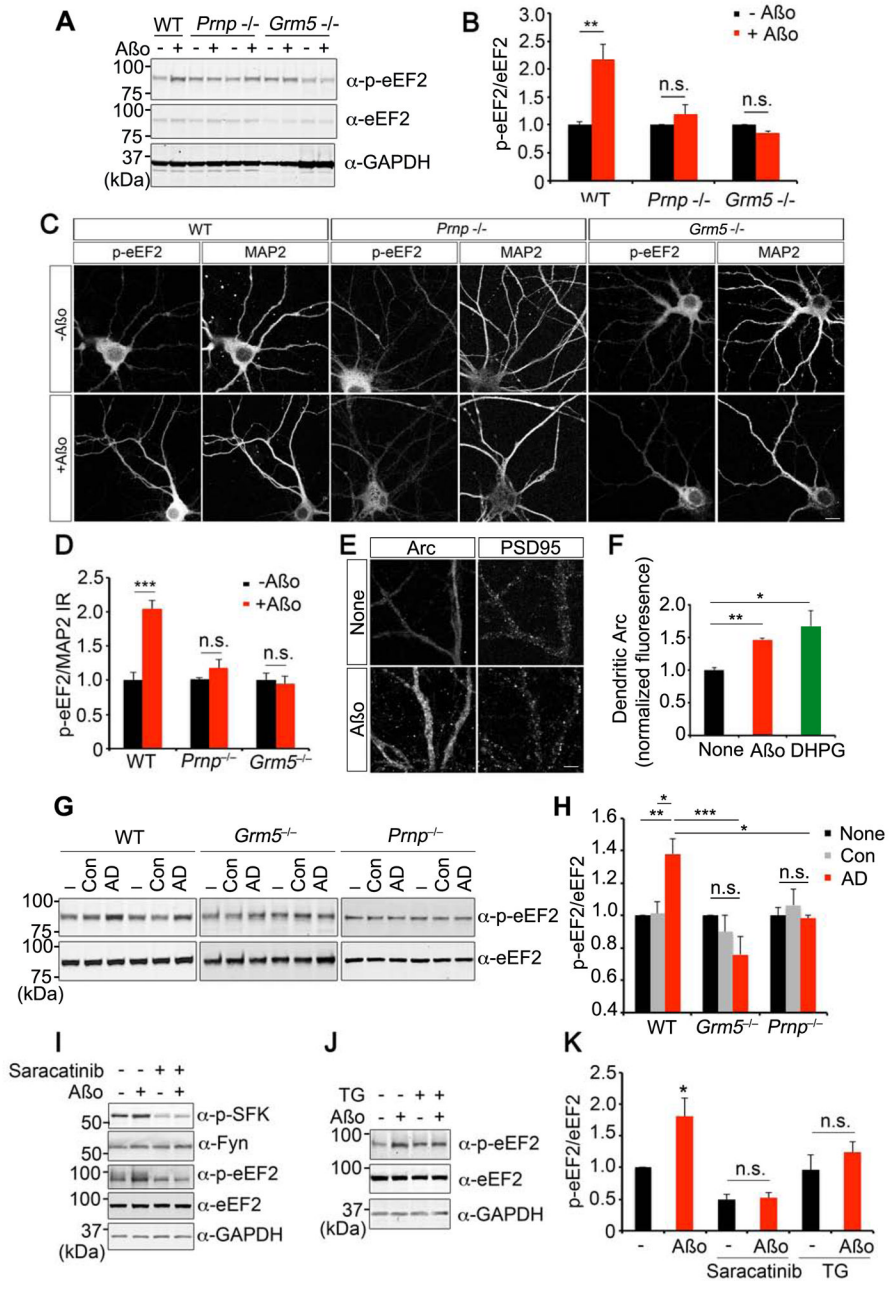

Figure 5. eEF2 phosphorylation is enhanced by Aβo through PrP and mGluR5

A DIV21 cortical neurons from WT, *Prnp*−/− or *Grm5*−/− mice were treated with 0 or 1 μM Aβo for 5 min. Lysates were analyzed by anti-phospho-eEF2, or anti-eEF2 immunoblot. GAPDH is loading control.

B Phospho-eEF2 level in the lysate normalized to eEF2. WT, n=3; *Prnp*−/−, n=3; *Grm5*−/−, n=3. Mean±sem, **, $P<0.01$; Student's two-tailed *t* test.

C Immunohistology of DIV21 WT, *Prnp*−/− or *Grm5*−/− cortical neurons stained with anti-phospho-eEF2 and anti-MAP2 antibodies after exposure of 0 or 1 μM Aβo. Scale bar, 10 μm.

D Phospoho-eEF2 intensity normalized to MAP2 signal. WT, n=3; *Prnp*−/−, n=3; *Grm5*−/−, n=3. 8–10 images were analyzed per experiment. Mean±sem, ***, $P<0.001$; Student's two-tailed *t* test.

E Immunohistology of DIV 21 WT neurons stained with anti-Arc antibody after 1 μM Aβo for 5 min. Scale bar, 5 μm.

F Arc intensity in dendrites after 1 μM Aβo or 100 μM DHPG for 5 min. For dendritic Arc levels, average pixel intensity was measured in secondary dendrites 10 μm from first branch point. WT, n=6. Mean±sem, **, $P<0.01$, *, $P<0.05$; ANOVA, Tukey post-hoc pairwise comparisons.

G DIV21 cortical neurons from WT, *Grm5*−/− or *Prnp*−/− mice were treated with human control or AD brain extracts (30 μg total protein/ml) for 5 min. Lysates were analyzed by anti-phospho-eEF2 or anti-eEF2 immunoblot.

H Phospho-eEF2 level normalized to eEF2 from G. WT, n=6; *Grm5*−/−, n=4; *Prnp*−/−, n=3. Mean±sem, *, $P<0.05$; **, $P<0.01$; ***, $P<0.001$; ANOVA, Tukey post-hoc pairwise comparisons.

I, J WT cortical neurons were treated with 0 or 1 μM Aβo for 15 min. Indicated samples were treated with 500 nM saracatinib for 1 hour (I) or 100 nM thapsigargin (TG) for 24 hours (J) prior to Aβo. Lysates were analyzed by anti-phospho-SFK, anti-Fyn, anti-phospho-eEF2, or anti-eEF2 immunoblot. GAPDH is loading control.

K Phospho-eEF2 level normalized to eEF2 from 3 experiments. Mean±sem, *, $P<0.05$; ANOVA, Tukey post-hoc pairwise comparisons.

See also Fig. S5.

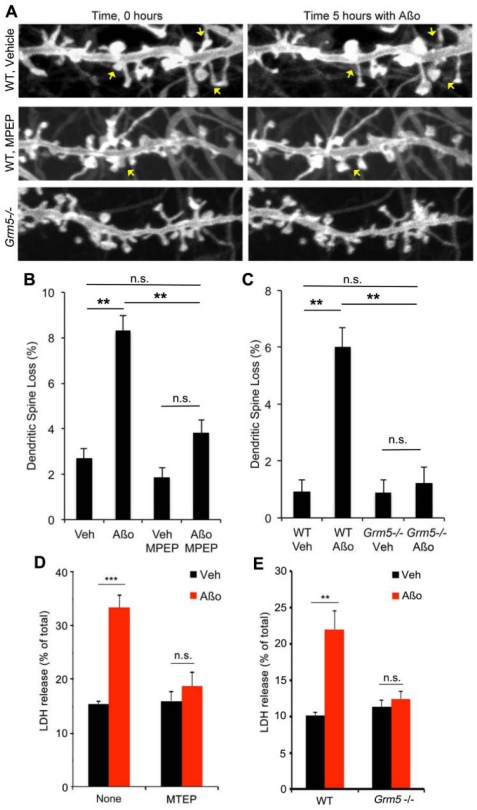

Figure 6. Aβo-induced toxicity is blocked by mGluR5 antagonists

A Hippocampal neurons (21DIV) expressing myristoyl-GFP from WT or *Grm5−/−* mice were imaged for 6 h with or without MPEP (100 μM). Aβo (500 nM monomer equivalent) or vehicle was added at 1 h. Note loss of several spines after Aβo addition in the WT neurons. Scale bar, 1 μm.

B, C Dendritic spine loss over 5 hours is plotted as a function of Aβo and MPEP (B) or *Grm5* genotype (C). Mean±sem, n=3–5 cultures from separate mice of each genotype. *, $P<0.05$; **, $P<0.01$; ANOVA, Tukey post-hoc pairwise comparisons.

D Neurons at DIV21 from WT mice were treated with 0 or 1 μM Aβo for 2 h. Some cultures were treated with 100 μM MTEP for 1 h prior to Aβo. Cell toxicity was determined by LDH release. Mean ± sem, n=3 experiments. ***, $P<0.001$; ANOVA, Tukey post-hoc pairwise comparisons.

E WT or *Grm5−/−* cortical neurons were treated with 0 or 1 μM Aβo for 2 h. Toxicity was determined by LDH release. Mean±sem, n=4 experiments. **, $P<0.01$; ANOVA, Tukey post-hoc pairwise comparisons.

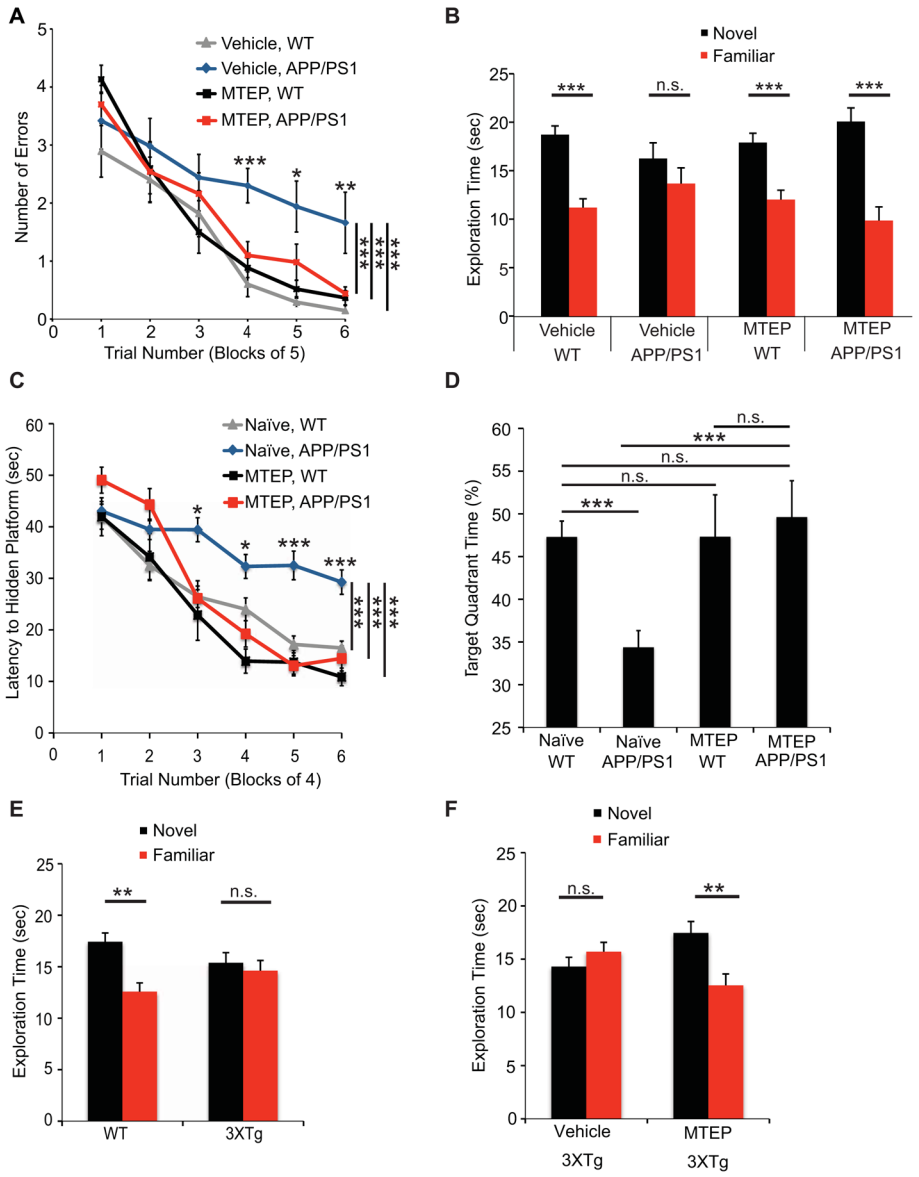

Figure 7. mGluR5 Antagonist Reverses Learning and Memory Deficits in AD Mouse Models

A Spatial learning is plotted as the number of errors in finding a hidden platform in a radial arm water maze at age 9 months. Mean±sem for vehicle treated C57BL/6, n=11; MTEP treated C57BL/6, n=12; vehicle treated APP/PS1, n=10; MTEP treated APP/PS1, n=10. Performance differed across the last 15 swims by genotype and treatment (two-way RM-ANOVA APP/PS1, $P<0.001$; MTEP, $P<0.001$). There was an interaction between genotype and treatment (two-way RM-ANOVA APP/PS1xMTEP $P<0.001$). By Tukey post-hoc pairwise comparisons across trials, the vehicle-treated APP/PS1 group differed from each of the other groups ($P<0.001$), while none of the other groups differed from each other ($P>0.05$). For indicated trial blocks, the vehicle-treated APP/PS1 group differed from each of the other groups (*$P<0.05$; **$P<0.01$; ***$P<0.001$), while none of the other groups differed from each other ($P>0.05$).

B Time spent with a novel object for the same mice as A: vehicle C57BL/6, n=11; MTEP C57BL/6, n=12; vehicle APP/PS1, n=9; MTEP APP/PS1, n=9. After being acclimated to an

object, vehicle APP/PS1 mice showed no preference for a novel object (two tailed Student's *t* test $P>0.05$). The other 3 groups showed preference for a novel object (two tailed Student's *t* test $P<0.001$).

C Spatial learning is plotted as latency to find a hidden platform in a Morris water maze at age 9 months in a cohort different from A. Mean±sem for untreated (naïve) C57BL/6, n=32; MTEP treated C57BL/6, n=13; untreated APP/PS1, n=38; MTEP treated APP/PS1, n=17. Performance differed across the last 16 swims by genotype and treatment (two-way RM-ANOVA for APP/PS1, $P<0.001$; for MTEP, $P<0.001$). There was an interaction between genotype and treatment (two-way RM-ANOVA, APP/PS1xMTEP $P<0.001$). By Tukey post-hoc pairwise comparisons across trials, the vehicle-treated APP/PS1 group differed from each of the other groups (***$P<0.001$), while none of the other groups differed from each other ($P>0.05$). For specific trial blocks, the untreated APP/PS1 group differed from each of the other groups (*$P<0.05$; ***$P<0.001$), while none of the other groups differed from each other ($P>0.05$).

D Performance during a 60 sec probe trial, 24 h after learning, where time spent in the target quadrant was measured. Random chance is 25%. Mean±sem for the groups in C. Target quadrant time differed by genotype and treatment (two-way ANOVA APP/PS1, $P<0.001$; MTEP, $P<0.01$). There was an interaction between genotype and treatment (ANOVA, APP/PS1xMTEP $P<0.001$). By Tukey post-hoc, the untreated APP/PS1 group differed from others ($P<0.001$), while none of the other groups differed from each other ($P>0.05$).

E WT and 3XTg mice of the same genetic background at 8–9 months of age were tested for novel object recognition. WT mice show preference the novel object (two-tailed Student's *t* test $P<0.05$), but 3XTg mice show no preference ($P>0.05$). Mean±sem.

F The effect of MTEP administration on object recognition is tested in 3XTg mice at age 8 months. Mean±sem for vehicle 3XTg, n=12; MTEP 3XTg, n=8. Mice that received MTEP had a significant preference for the novel object (two tailed Student's *t* test $P<0.01$) while vehicle 3XTg mice showed no preference (two-tailed Student's *t* test $P>0.05$).

See also Fig. S6.

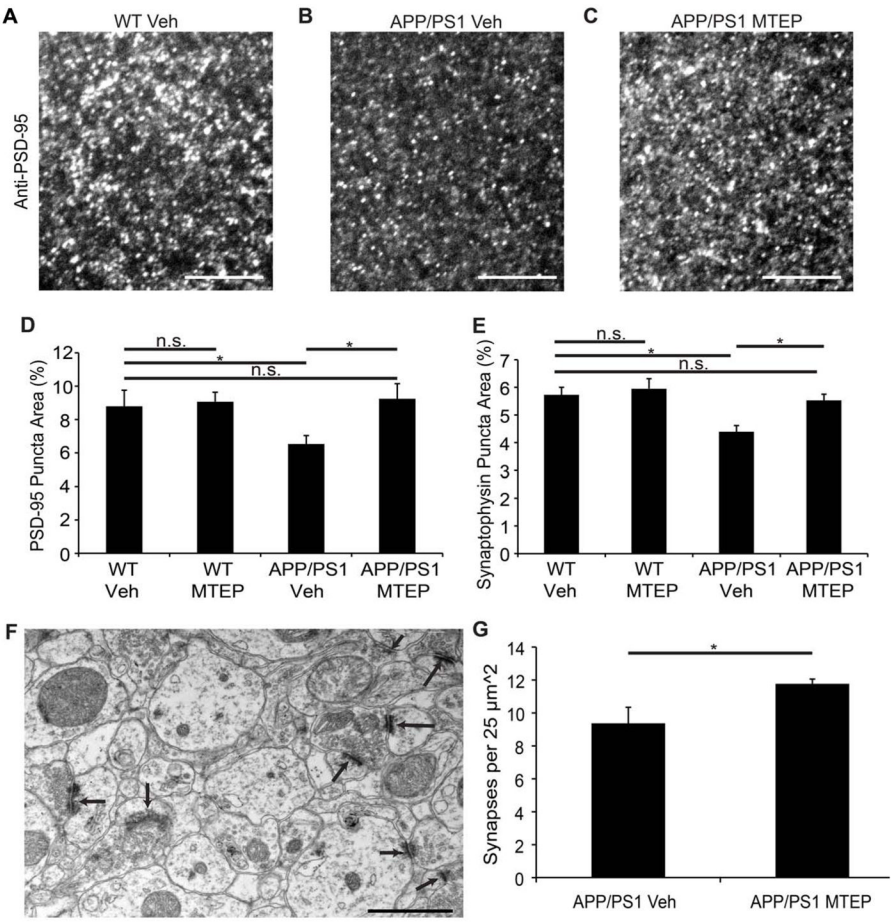

Figure 8. Synaptic Markers Recover After 10-Day Treatment With mGluR5 Antagonist

WT and APP/PS1 mice at 10 months of age were treated with 15 mg/kg of MTEP, or saline, by intraperitoneal injection twice a day for 10 days and then sacrificed for histological analysis.

A–C The molecular layer of the dentate gyrus of the indicated groups was stained with anti-PSD-95 antibody and imaged with a confocal microscope and a 60X objective lens. Scale bar, 6 μm.

D Fractional area of immunoreactive puncta for PSD-95 from images as in A–C. $P<0.05$, ANOVA with post-hoc pairwise LSD. Mean±sem, n=5 mice per group with 3 images per mouse.

E Fractional area of immunoreactive puncta for synaptophysin. $P < 0.05$, ANOVA with post-hoc pairwise LSD. Mean±sem, for n=5 mice per group with 3 images per animal.

F Ultrastructure of the molecular layer of the dentate gyrus from a vehicle APP/PS1 mouse. Arrows point to synapses scored in G. Magnification is 20,500X. Scale bar, 1 μm.

G Synapses were counted in a 25 μm^2 area in drug-treated and saline-treated samples. $P<0.05$, two-tailed Student's *t* test. Mean±sem, n=5 mice per group with 30 images per mouse.